Carboxylates versus Fluorines: Boosting the Emission Properties of Commercial BODIPYs in Liquid and Solid Media

Gonzalo Durán-Sampedro, Antonia R. Agarrabeitia, Luis Cerdán, M. Eugenia Pérez-Ojeda, Angel Costela, Inmaculada García-Moreno, Ixone Esnal, Jorge Bañuelos, Iñigo López Arbeloa, and María J. Ortiz**

A new and facile strategy for the development of photonic materials is presented that fufills the conditions of being efficient, stable, and tunable laser emitters over the visible region of spectrum, with the possibility of being easily processable and cost-effective. This approach uses poly(methyl methacrylate) (PMMA) as a host for new dyes with improved efficiency and photostability synthesized. Using a simple protocol, fluorine atoms in the commercial (4,4-difluoro-4-bora-3a,4a-diaza-s-indacene) (*F*-BODIPY) by carboxylate groups. The new *O*-BODIPYs exhibit enhanced optical properties and laser behavior both in the liquid and solid phases compared to their commercial analogues. Lasing efficiencies up to 2.6 times higher than those recorded for the commercial dyes are registered with high photostabilities since the laser output remain at 80% of the initial value after 100 000 pump pulses in the same position of the sample at a repetition rate of 30 Hz; the corresponding commercial dye entirely loses its laser action after only 12 000 pump pulses. Distributed feedback laser emission is demonstrated with organic films incorporating new *O*-BODIPYs deposited onto quartz substrates engraved with appropriated periodical structures. These dyes exhibit laser thresholds up to two times lower than those of the corresponding parent dyes with lasing intensities up to one order of magnitude higher.

1. Introduction

Presently, the development of photonic materials fulfilling the conditions of being efficient, stable and tunable emitters over the visible region of the electromagnetic spectrum, with the possibility of being easily processable, and cost-effective, is an area of active research driven by the wide range of possible practical applications. Over the last years, a vast amount of work has been carried out on materials engineering, designing and synthesizing semiconductor polymers and organic, hybrid and inorganic systems nano- and mesostructured, doped with organic dyes and quantum dots.[1] Nevertheless, despite this extensive activity up to now none of the obtained materials happens to meet all the above requirements at the same time.

Our research group has contributed greatly to this effort, developing solid state dye lasers (SSDL) both in bulk matrices and waveguiding thin films, on the basis of organic and/or hybrid materials doped with dyes with emission covering the spectral region from 550 up to 730 nm.[2] Albeit we have demonstrated lasing efficiencies as high as 60% in some particular case, the materials we have developed exhibit on average efficiencies of about 30% with photostabilities that being higher than those reported by other researchers, demand nonetheless an improvement in order to guarantee the implementation of these materials in practical applications. In addition, our work has shown that there is not an universal material that optimizes the lasing behavior of all the different dyes, but that a specific dye/host combination is needed for each chromophore, which is determined by the photophysical and photochemical chromophore's properties.

Here, we propose a new and facile strategy for the development of laser materials economically affordable with optimized emission properties in the visible region of the spectrum. This approach implies the utilization of a commercial polymer (poly(methyl methacrylate), PMMA) competitive in cost and easily processable, as host for dyes with improved efficiency and photostability. The chromophores are new derivatives of a

G. Durán-Sampedro, Prof. A. R. Agarrabeitia, Prof. M. J. Ortiz
Departamento de Química Orgánica I
Facultad de Ciencias Químicas
Universidad Complutense
28040, Madrid, Spain
E-mail: mjortiz@quim.ucm.es
Dr. L. Cerdán, M. E. Pérez-Ojeda, Prof. A. Costela, Prof. I. García-Moreno
Departamento de Sistemas de Baja Dimensionalidad Superficies y Materia Condensada
Instituto Quimica-Fisica "Rocasolano"
C.S.I.C., Serrano 119, 28006 Madrid, Spain
E-mail: i.garcia-moreno@iqfr.csic.es
I. Esnal, Dr. J. Bañuelos, Prof. I. López Arbeloa
Departamento de Química Física
Facultad de Ciencias y Tecnología
Universidad del País Vasco-EHU
Apartado 644, E-48080-Bilbao, Spain

DOI: 10.1002/adfm.201300198

single family of commercial dyes obtained following a simple and general synthesis protocol, which exhibits high reaction yields. The selected family of dyes was that of the so-called *F*-BODIPYs (4,4-difluoro-4-bora-3a,4a-diaza-*s*-indacene), developed in the late 1980s and early 1990s by Boyer and co-workers, because they exhibit high fluorescence quantum yields, intense absorption, and tunable emission wavelength[3] as well as high chemical versatility to be functionalized.[2b,4] Currently, these dyes have numerous applications such as fluorescent probes in biological systems, photosensitizers for photodynamic therapy, and as materials for incorporation into electroluminescent devices.[5]

Among the numerous modifications in the BODIPY core, the replacement of one or both of the fluorine atoms in *F*-BODIPYs has become an active area. Thus, a wide variety of BODIPY dyes have been synthesized via fluorine displacement by alkyl or aryl derivatives (*C*-BODIPY),[5a–c,6] ethynyl groups (*E*-BODIPY),[5a–c,6e,7] and alkoxy or aryloxy derivatives (*O*-BODIPY),[5a–c,6c,6f–g,8] including *O*-chelated BODIPYs.[9] In addition, new types of boron modifications as borenium cations,[10] *CN*-BODIPY,[6a] *H*-BODIPY[10] and *Cl*-BODIPY,[6d,6g–h] have also been reported.

In one recent publication the authors evaluated the replacement of one or both of the fluorine atoms in 4,4-difluoro-1,3,5,7-tetramethyl-4-bora-3a,4a-diaza-*s*-indacene by acetoxy (AcO) groups in order to study the effect of an electron-withdrawing carboxylate on the boron atom in BODIPY, and they found that mono- and di-AcO substituted BODIPYs exhibited excellent fluorescence quantum yields and photostabilities.[11] Furthermore, the AcO modification on boron resulted in significantly improved water solubility, which is highly desirable for biological applications.[11] In another report about the stability of the BODIPY fluorophore under acidic and basic conditions, a 4,4-dichloroacetoxy BODIPY was formed when 4,4-dimetoxi-2,6-diethyl-1,3,5,7-tetramethyl-4-bora-3a,4a-diaza-*s*-indacene was mixed with an excess of dichloroacetic acid in CH_2Cl_2.[6f] However, no fluorescence study of this compound was explored.

Based on these observations, in the present work we report the synthesis and emission properties characterization of a library of *O*-BODIPYs **1**–**10** (**Figure 1**) from commercially available BODIPYs, in which two carboxylate (acetoxy or trifluoroacetoxy) groups are connected to the boron center in the place of the fluorine atoms. It is shown that these dyes are highly fluorescent and exhibit enhanced laser action with respect to their *F*-BODIPY analogues, both in liquid solution and solid phase. To investigate in depth the influence of the acetoxy substitutions on the BODIPY emission properties we have also synthesized, as a proof of concept, new *O*-BODIPYs via fluorine displacement by other carboxylate groups with different electronic character such as acryloyloxy, propioloyloxy, methoxy, or 4-nitrophenoxy groups (**11–14**).

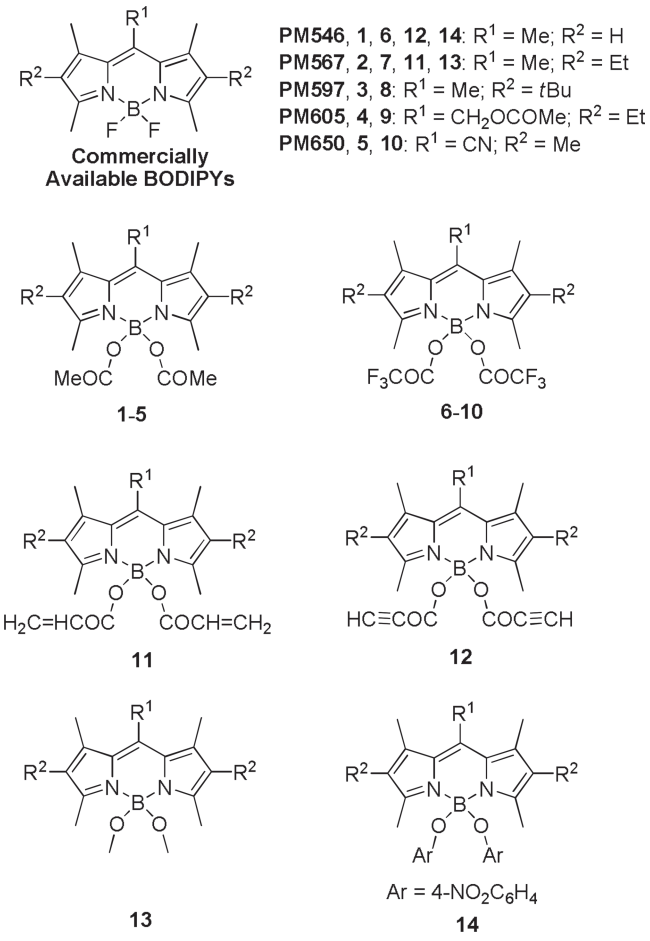

Figure 1. Molecular structures of dyes synthesized herein and their parent dyes.

2. Results and Discussion

2.1. Synthesis

BODIPY dyes **1**–**14** were successfully obtained from commercially available dyes[12] PM546, PM567, PM597, PM605 and PM650 through nucleophilic substitution reactions of fluorine atoms in the BF_2-group. Thus, 4,4-diacetoxy BODIPYs **1**,**2**,**4** and **5** were prepared with moderate yields by treating 20 equiv of TMSOAc with 1 equiv of PM546, PM567, PM605 or PM650, respectively, in presence of 3-4 equiv of $AlCl_3$ as Lewis acid (method A). In all these cases the monosubstituted derivative is not isolated. The dye **3** could not be synthesized by this method, so that an alternative procedure (method B) was used for their preparation involving the generation in situ of TMSOAc from acetic acid and TMSCl, in the absence of $AlCl_3$. Method B was also used in the synthesis of 4,4-bis(trifluoroacetoxy) BODIPYs **6**,**7** and **9** by adding of $TMSOCOCF_3$, generated in situ from trifluoroacetic acid and TMSCl, to the BODIPYs PM546, PM567 and PM605, respectively. 4,4-Bis(acryloyloxy) BODIPY **11** was prepared by reacting of PM567 with $TMSOCOCH=CH_2$, generated in situ from acrylic acid and TMSCl (method B), and this same method was used in the preparation of **12** from PM546 with propargylic acid and TMSCl. **Scheme 1** shows the synthesis of the dyes **2**,**7** and **11** from commercial BODIPY PM567.

Surprisingly, treatment of PM597 with $TMSOCOCF_3$ in 1,2-dichloroethane resulted in a mixture of **15** (10%) and **6** (22%) by loss of one or both *terc*butyl groups present in the starting compound (**Scheme 2**). Therefore, we were decided to develop an alternative procedure (method C). Thus, BODIPY**8**

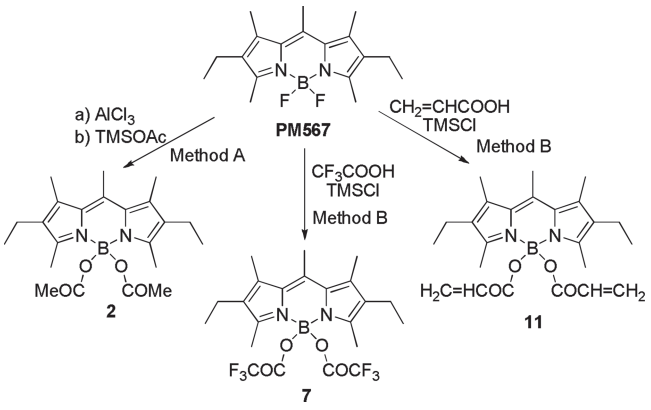

Scheme 1. Synthetic routes of derivatives **2**, **7**, and **11** from parent dye PM567.

was achieved by treatment of BODIPY PM597 with $AlCl_3$ in 1,2-dichloroethane and subsequent addition of $TMSOCOCF_3$, generated in situ as above (Scheme 2). Similarly, compound **10** was successfully obtained from PM650 with moderate yield.

In addition, two other analogues, 4,4-dimethoxy **13**,[6f] and 4,4-bis(4-nitrophenyl) **14** were synthetized according to procedure described in the literature or through the method A mentioned above.

2.2. Photophysical Properties

The selected commercial BODIPY laser dyes span a wide region of the visible spectrum; hence, the emission can be tuned from the green-yellow to the red as it is illustrated in **Figure 2**. The progressive bathochromic shift of the spectral bands is due to inductive donor effects of the alkyl groups at positions 2 and 6 (PM567 and PM597 vs PM546) or the electron withdrawing character of methylenacetoxy (PM605) or cyano (PM650) groups at position 8, which lead to a net stabilization of the LUMO molecular orbital.[4a] Except for the PM650 derivative, where a fluorescence quenching intramolecular charge transfer state is operative,[4a] these BODIPYs outstand by their bright and stable emission. For this reason, the set of derivatives from PM650 will be discussed later on.

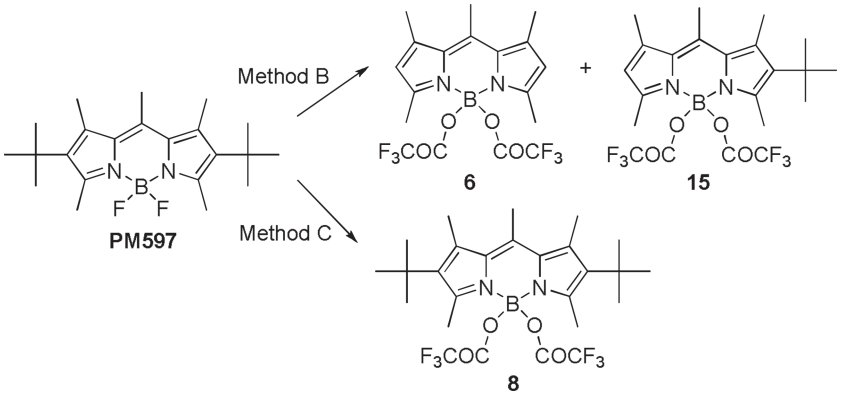

Scheme 2. Synthetic routes of derivatives **6**, **8**, and **15** from parent dye PM597.

At first sight, the replacement of the fluorine atoms by alcoxy or aryloxy derivatives should have minor influence on the photophysical properties of the chromophore since the BF_2 group does not take part in the delocalized π-system and acts as a bridge to keep the planarity and rigidity of the indacene core. For this reason, as is shown in **Table 1**, the positions of the spectral bands of the new *O*-BODIPYs are almost those of their respective *F*-BODIPY counterparts. Besides, the solvent effect on the photophysical properties follows the normal trends previously described for *F*-BODIPYs (Table S1–S4 in the Supporting Information); i.e., small hypsochromic spectral shifts with the solvent polarity and low dependency of the fluorescence quantum yield with the solvent characteristics.

Moreover, and as a common rule except for the dyes **13** and **14** that will be discussed later on, the fluorescence quantum yield and lifetime of the new *O*-BODIPYs increase with respect to the commercial ones, ameliorating the emission properties of the commercial *F*-BODIPYs, which were considered as a benchmark in fluorescence and laser behavior in the middle energetic part of the visible spectrum (Table 1).[6b,11] The enhancement of the emission properties of the *O*-BODIPYs depends on the electronic character of the carboxylate groups connected to the boron center in the following manner: while the fluorine displacement by the electron withdrawing acetoxy group (**1-4**) maintains or slightly improves the high fluorescent ability of the BODIPYs, a further increase in the electron acceptor character of the substituent via the inclusion of trifluoroacetoxy groups (**6–9**) leads to an even more significant improvement on the fluorescence quantum yield, which reaches nearly the unit in some solvents. Moreover, the same statement holds true for the attachment of other electron withdrawing carboxylate groups, such as acryloyloxy (**11**) or propioloyloxy (**12**).

It is noteworthy to remark the important improvement achieved in the fluorescent efficiency of PM597 through the replacement of fluorine atoms by carboxylate groups, thus, its fluorescence quantum yield increases from 0.43 up to 0.58 and 0.76 for its **3** and **8** *O*-BODIPYs derivatives, respectively (Table 1). The photophysical properties of the parent PM597 are controlled by the sterical hindrance induced by the *tert*-butyl groups at positions 2 and 6, which twists the planarity of the chromophore leading to an increase of both the internal conversion probability and the Stokes shift with respect to other planar BODIPYs such as, for instance, PM567. The **3** and **8** derivatives exhibit lower non-radiative rate constant than PM597, which could be related to the influence of the carboxylate group in the molecular geometry.

Overall, quantum mechanics calculations predict that the carboxylates are symmetrically disposed up and down the indacene core, both in the ground and excited state (**Figure 3**). Whereas the planarity of most of the *O*-BODIPYs remains the same regarding to their parent *F*-BODIPYs, a slight increase in the planarity is predicted for the PM597 derivatives since the dihedral angles, accounting for the pyrrole disposition with respect to the central ring, increase in around 3° in the excited state. However,

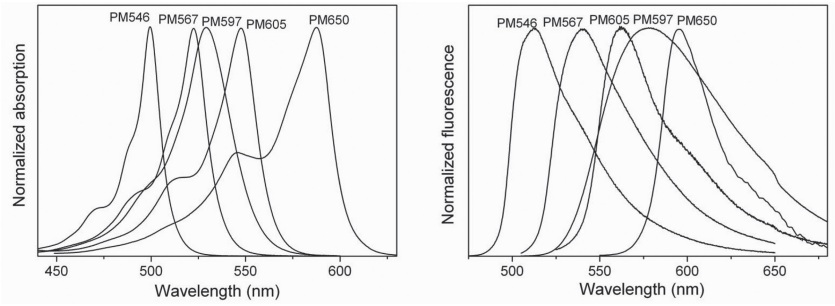

Figure 2. Normalized absorption and fluorescence spectra of commercial *F*-BODIPYs in a common solvent (cyclohexane).

such enhancement seems to be not strong enough to explain the important reduction observed in the internal conversion processes upon displacement of fluorine by carboxylate in the PM597 dye.

On the other hand, the photophysics behavior of the new *O*-BODIPY dyes depends strongly on the electronic character of the carboxylates substituent. Thus, the replacement of fluorine in PM567 by an electron donor methoxy group (**13**) has the opposite effect on the photophysical behavior with respect to that induced by electron withdrawing carboxylates since the presence of the–OCH_3 groups leads to a small reduction in the fluorescence quantum yield of the chromophore.

The opposite influence of the carboxy groups in the fluorescence quantum yield depending on their electronic character was analyzed in terms of the charge distribution in the corresponding excited states (Figure S1–S4 in the Supporting Information). In fact, the linkage of carboxylates to the boron atom implies a rearrangement in the chromophoric charge distribution, as it is reflected for PM567 in Figure 3. The acetoxy group behaves as an electron acceptor group (Hammet parameter, $\sigma_p = 0.31$).[13] Thus, its attachment to the boron leads to an increase of the positive charge in this last atom, while the oxygen acquires a negative charge much higher than of the fluorine in the corresponding *F*-BODIPYs. Such trend is more pronounced as the electron withdrawing character of the carboxylate substituent increases, for instance, in the case of the trifluoroacetoxy group (σ_p = 0.46). However, the replacement of fluorine atoms by electron donor methoxy groups (σ_p = –0.27) leads to the opposite behavior; the positive charge in the boron atom decrease and the oxygen results less negatively charged (Figure 3).

This rearrangement of the electronic charges around the boron atom determines the charge distribution of the chromophore (usually described as a cyclic cyanine). In fact, the negative charge of the aromatic nitrogen atoms decreases upon the presence of carboxylate groups (Figure 3 and Figure S1–S4 in the Supporting Information). This trend suggests that the electron lone pair is less localized in the nitrogen and tends to be more delocalized through the cyanine system. Furthermore, the charge alternation is softened, which is also indicative of higher delocalization. In addition, the aromatic character of the chromophore can be roughly evaluated by means of the Bond Length Alternation (BLA) parameter, which is defined as the difference between the average carbon-carbon bond lengths of alternative single and double bonds in the chromophoric π-system.[14] Regarding the corresponding values for

Table 1. Photophysical properties of commercial *F*-BODIPYs (PM546, PM567, PM597 and PM605) and their corresponding *O*-BODIPYs in cyclohexane; absorption (λ_{ab}) and fluorescence (λ_{fl}) wavelength at the maximum, Stokes shift ($\Delta\nu_{St}$), molar absorption at the maximum (ε_{max}), fluorescence quantum yield (φ) and lifetime (τ), and radiative (k_{fl}) and non-radiative (k_{nr}) rate constants. The full photophysical data in several media are collected in the Supporting Information (Table S1–S4).

	λ_{ab} [nm]	ε_{max} [$10^{-4}M^{-1}cm^{-1}$]	λ_{fl} [nm]	$\Delta\nu_{St}$ [cm^{-1}]	φ	τ [ns]	k_{fl} [10^{-8} s^{-1}]	k_{nr} [10^{-8} s^{-1}]
PM546	499.5	9.7	509.5	400	0.91	5.23	1.74	0.17
1	501.0	9.5	508.0	275	0.91	5.40	1.68	0.17
6	502.0	10.2	509.5	295	0.95	5.52	1.72	0.10
12	502.0	8.2	511.0	350	0.99	5.62	1.76	0.02
14	499.5	11.6	511.0	450	0.89	5.94	1.50	0.18
PM567	522.5	9.3	537.0	520	0.88	5.60	1.57	0.21
2	522.0	8.5	537.0	535	0.84	5.71	1.47	0.28
7	525.5	7.8	541.5	565	0.94	6.25	1.50	0.10
11	523.5	8.1	541.0	620	0.90	5.98	1.50	0.17
13	522.0	8.0	539.5	620	0.81	5.64	1.44	0.34
PM597	529.0	8.1	571.0	1395	0.43	3.91	1.10	1.46
3	530.5	7.0	573.0	1400	0.58	4.58	1.27	0.92
8	532.5	5.4	571.0	1265	0.76	5.99	1.27	0.40
PM605	547.5	8.6	561.0	435	0.74	6.27	1.18	0.41
4	548.5	8.0	563.0	470	0.76	6.37	1.19	0.38
9	551.0	7.8	564.0	420	0.80	6.99	1.14	0.28

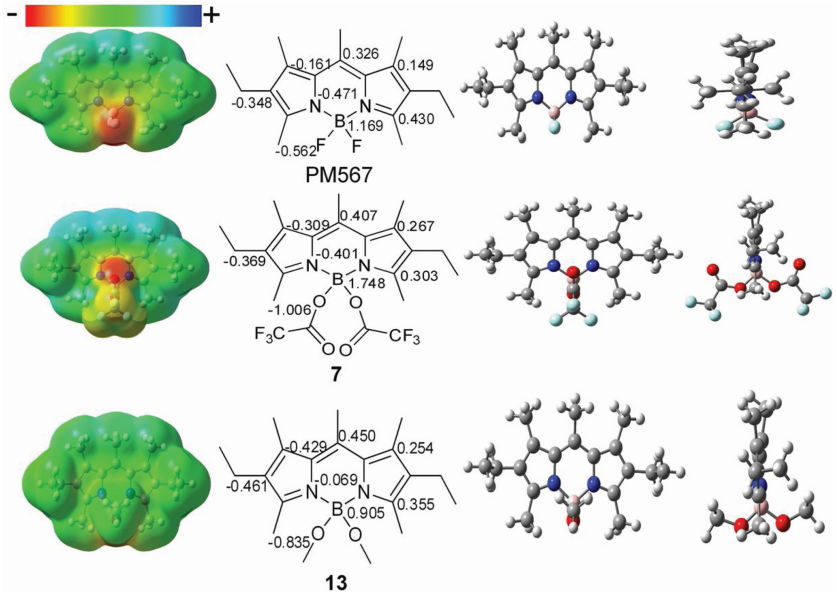

Figure 3. Electrostatic potential maps, ChelpG charge distribution (the corresponding data for the symmetrical counterpart in the chromophore are not included) in the excited state and the corresponding excited state geometries (at two different views) for PM567 dye and its derivatives **7** (trifluoroacetoxy) and **13** (methoxy). The electronic density distributions for all the derivatives are collected in Figure S1–S5 in the Supporting Information.

the *F*-BODIPYs and their respective *O*-BODIPYs, listed in Figure S1-S4 in the Supporting Information, the BLA parameter for dyes bearing acetoxy groups remains similar to that of their parent BODIPY (i.e., compound **2** (0.0227) vs PM567 (0.0222), in Figure S2, Supporting Information), but decreases for the derivatives bearing trifluoroacetoxy groups (i.e., compound **7** (0.0192) in Figure S2, Supporting Information). This tendency of the BLA parameter points out a higher aromaticity of the chromophore induced by the presence of electron withdrawing carboxylates, in good concordance with the enhancement of the fluorescence quantum yield experimentally observed. However, the presence of methoxy groups with electron donor character leads to an enhancement in the BLA parameter (0.0260 for compound **13** in Figure S2, Supporting Information) in line with the recorded decrease in the fluorescence efficiency. This evolution is even more pronounced for the PM597 derivatives **3** and **8** (0.0225, 0.0217 and 0.0181, respectively in Figure S3 in the Supporting Information). This fact, together with the slight increase in its planarity, could explain why this dye is the most sensitive system to the fluorine replacement by carboxylates.

On the other hand, aryloxy groups (4-nitrophenoxy) have also been attached to the boron of PM546 (compound **14**), replacing the fluorine atoms. While in apolar solvents the fluorescence efficiency keeps similar to the parent PM546 (Table 1), an increase in the polarity of the surrounding environment implies a progressive decrease of the fluorescence quantum yield, becoming almost negligible in the most polar solvents (from 0.89 in c-hexane to 0.05 in F_3-ethanol, Table S1 in the Supporting Information). At the same time, as is reflected in **Figure 4**, the fluorescence decay gets faster and eventually biexponential with a dominating lifetime of 0.18 ns, which reaches a contribution higher than 97% in F_3-ethanol (Table S1 in the Supporting Information). The presence of such fast lifetime indicates the presence of an extra non-radiative deactivation pathway, which is getting a higher influence as the solvent polarity increases and leads to very low fluorescence quantum yield in those media, in contrast to the rest of related *O*-BODIPYs where the fluorescence efficiency remains almost constant regardless of the solvent properties. Such fluorescence quenching in compound **14** and mainly in polar media suggests the activation of an intramolecular charge transfer (ICT) state from the BODIPY core to the nitro group, which is characterized by its strong electron withdrawing ability (σ_p = 0.78). In fact, the presence of ICT states induced by the direct attachment of nitro groups to the BODIPY core have been previously reported.[15] Therefore, although we have concluded before that the replacement of fluorine by electron withdrawing alcoxys

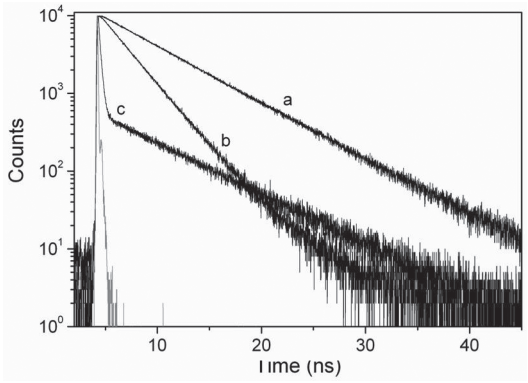

Figure 4. Fluorescence decay curves of compound **14** in a) cylochexane, b) methanol, and c) trifluoroethanol.

Table 2. Photophysical properties of the PM650 and its corresponding *O*-BODIPYs (**5** and **10**) in cyclohexane and methanol. The full photophysical data in several media are collected in Supporting Information (Table S5).

	λ_{ab} [nm]	ε_{max} [$10^{-4}M^{-1}cm^{-1}$]	λ_{fl} [nm]	$\Delta\nu_{St}$ [cm^{-1}]	φ	τ [ns]	k_{fl} [10^{-8} s^{-1}]	k_{nr} [10^{-8} s^{-1}]
PM650								
c-hexane	589.5	5.3	599.5	290	0.36	4.67	0.77	1.37
Methanol	587.5	4.1	609.0	605	0.060	1.29	0.46	7.29
5								
c-hexane	588.5	4.5	600.5	340	0.39	5.19	0.75	1.17
Methanol	589.0	3.7	610.0	585	0.073	1.54[a)]	0.47	6.02
10								
c-hexane	591.0	3.8	599.0	225	0.47	5.99	0.78	0.88
Methanol	591.0	2.7	609.5	515	0.11	2.23	0.49	3.99

[a)]Main component (>98%) of the biexponential fit of the decay.

ameliorates the fluorescence of the dye, if the electron acceptor capacity of these substituent groups is too high, it could give rise to an extra non-radiative pathway (ICT), which quenches the fluorescence emission mainly in polar media.

Whereas all the above commented *F*-BODIPYs, were characterized by a bright fluorescence regardless of the media, the emission properties of the PM650 are limited by the presence of an ICT state induced by the electron withdrawing cyano group (σ_p = 0.66) attached at position 8 (in a similar way to compound **14**).[4a] Thus, the fluorescence efficiency of this fluorophore, especially in polar solvents, is lower than that exhibited by other commercial BODIPYs (**Table 2** and Figure S5 in the Supporting Information). Furthermore, it was previously reported the unstability of PM650 dye in certain solvents (most of them characterized as electron donors)[16] since its solutions were completely bleached after some hours or days, depending of the solvent nature, as result of a specific interaction of the cyano group and those solvents. For this reason, all data listed for the derivatives of PM650 have been registered just after sample preparation.

In general, the replacement of the fluorine by carboxylates in PM650 follows the above commented trends for alkylated BODIPYs; thus, the presence of acetoxy (**5**) and mainly trifluoroacetoxy (**10**) improves the fluorescence capacity of the dye (Table 2). However, the presence of the quenching ICT process limits the fluorescence performance of these derivatives in polar media, and, although the fluorescence quantum yield is ameliorated it is still too low (around 0.1 in methanol in the best case, Table S5 in the Supporting Information) to achieve good laser performance. Whereas the presence of such quenching ICT state is harmful for the laser performance, it enables to apply PM650 and their O-BODIPYs derivatives as polarity sensors. The stabilization of the ICT state depends markedly of the solvent polarity, thus, the polarity of the surrounding environment can be monitored by means of the decrease in the fluorescence efficiency in such media or the change in the fluorescence colour (followed just with a naked eye) if the ICT state emits.[17] On the other hand, compounds **5** and **10** show also a lack of stability, even more pronounced than in the parent commercial PM650 and after few hours most of the solutions are bleached. Overall, the HOMO molecular orbital is stabilized when changing from *F*-BODIPYs to *O*-BODIPYs. Nevertheless, the carbon of the cyano gets a higher positive charge (from 0.463 in PM650 to 0.511 and 0.516 in compounds **5** and **10**, respectively, Figure S5 in theSupporting Information), whereas the nitrogen gets a slight higher negative charge. Therefore, the specific interaction of the cyano (through its carbon) with electron donor solvents should be more feasible in the *O*-BODIPYs, explaining its lower chemical stability than the reference PM650.

Summarizing, the replacement in the BODIPY core of fluorine atoms by electron withdrawing carboxylates is a good strategy to improve the fluorescence behavior, since it leads to more aromatic chromophores and, consequently, an enhanced laser action both in liquid and solid phase is expected.

2.2.1. pH-Dependence and Solubility Studies

To accomplish the characterization of the new *O*-BODIPYs their pH stability and water solubility were carefully studied. As a proof of concept, we detail the results achieved for the derivatives **1** and **6** related to the behavior exhibited by their parent dye PM546, under otherwise identical experimental conditions. The pH-dependence experiments of the BODIPY fluorophores **1** and **6** reveals that theses BODIPYs were less degraded in acidic and basic conditions than the commercial PM546 (Figure S6 in the Supporting Information). This behavior could be understand taking into account that the BF_2 bridge is the most labile position of the BODIPY and, consequently, it could be the most suitable position to be attacked by acids or bases. It seems that the charge redistribution around the boron atom (increase of its positive charge) upon the replacement of fluorine by carboxylates strengthens the ionic B–N bond leading to dyes more robust to extreme pHs. In fact, theoretical calculations predict a slight decrease in such bond length (except for PM650) from ≈1.54 to 1.51 induced by the presence of trifluoroacetoxy groups.

Moreover, a solubility study was carried out with the BODIPYs above mentioned. The results obtained show that compounds **1** and **6** are more soluble in water than the parent

Table 3 Lasing properties of commercial *F*-BODIPYs and their new derivatives at the dye concentrations that optimize their laser action in ethyl acetate solutions. [c]: dye concentration; Eff: lasing efficiency (ratio between the energy of the laser output and the pump energy incident on the sample surface); λ_l: peak wavelength of the laser emission; Intensity of the laser-induced fluorescence emission (I_n) after *n* pump pulses for dyes in ethyl acetate solution λ_{exc}: pumping wavelength.

	λ_{exc} = 355 nm, 5 Hz					λ_{exc} = 532 nm, 10 Hz													
	PM546	**1**	**6**	**12**	**14**	PM567	**2**	**7**	**11**	**13**	PM597	**3**	**8**	PM605	**4**	**9**	PM650	**5**	**10**
[c]/mM	2.5	3.8	7.5	2.5	2.5	1.5	1.5	0.6	1.5	9	0.5	0.9	0.9	0.6	0.6	0.6	0.9	1.4	0.5
Eff (%)	23	43	53	59	16	48	63	68	65	59	53	59	65	55	60	67	35	50	55
λ_l/nm	541	544	541	542	541	566	566	562	563	565	588	586	587	586	591	592	657	655	661
I_n (%) [a]	60	100	100	100	50	17	98	100	90	30	85	100	100	20	65	91	80	30	50
n/1000	100	100	100	100	100	100	100	100	100	100	100	100	100	40	70	100	100	50	70

[a] I_n (%) = 100 (I_n/I_0), with I_0 being the initial intensity.

PM546. Thus, while the PM546 is hydrophobic and it is not soluble in water, the dyes **1** and **6** exhibit 20 and 35 μg/mL, respectively, solubility in water, which is an important additional advantage of *O*-BODIPYs, in terms of their biological applications.

2.3. Lasing Properties

2.3.1. Liquid Phase

According to the absorption properties of the new BODIPYs (Table 1 and 2), their lasing properties were studied under pumping at 355 nm (dyes **1**,**6**,**12** and **14**, analogues of PM546) and 532 nm (all the other derivatives). Under our experimental conditions (transversal excitation and strong focusing of the incoming pump radiation) the concentration of the dyes should be in the millimolar range, to ensure total absorption of the pump radiation within the first millimeter at most of the solution, in order to obtain an emitted beam with near-circular cross-section and optimize the lasing efficiency (ratio between the energy of the dye laser output and the pump energy incident on the sample surface). To determine the dye concentration that optimizes the laser emission for the different derivatives, first the dependence of their laser emission on the corresponding dye concentrations was analyzed in ethyl acetate by varying the optical densities from 4 to 40, while keeping all the other experimental parameters constant. **Table 3** summarizes the concentrations that produced the highest lasing efficiencies in each case as well as the corresponding lasing wavelengths. It can be appreciated in Table 3 that in all cases the lasing efficiency of the derivatives is higher than that of the commercial parent dye, with the highest lasing efficiencies being obtained in the derivatives incorporating trifluoroacetoxy groups (**6–10**).

Following the photophysical analysis, the actual effect of the solvent on the dye laser action was analyzed in solutions of polar protic and polar aprotic solvents. Although the photophysical studies showed that the new derivatives exhibited their highest fluorescence capacity when dissolved in apolar solvent*c*-hexane, the low solubility of the synthesized *O*-BODIPYs in this solvent prevented preparation of solutions of the dyes in *c*-hexane at the concentration required for laser experiments under the pumping conditions selected in the present work. In all the other solvents, each dye was dissolved at the concentration that was found to optimize its emission in ethyl acetate (that is, the concentrations tabulated in Table 3).

In **Table 4** are presented the lasing properties of the new *O*-BODIPYs as a function of the solvent, together with those of the corresponding parent dyes. The lasing behavior of the new compounds is in good agreement with their photophysical properties (Table S1–S5 in the Supporting Information). In the acetoxy derivatives **1–4** the photophysics changes little in the different solvents and so does the lasing efficiency, which nevertheless improves in general that of the parent dyes, in accordance with the improvement of the fluorescence capacity of those derivatives with respect to the parent dyes.

As discussed in the previous section, the inclusion of the trifluoroacetoxy groups in the BODIPYs further enhanced the fluorescence capacity of the parent dyes. Correspondingly, derivatives **6–9** exhibit consistently higher lasing efficiencies

Table 4. Lasing efficiencies for the commercial *F*-BODIPY dyes and their new derivatives in different solvents. λ_{exc}: pumping wavelength.

Solvent	λ_{exc} = 355 nm					λ_{exc} = 532 nm													
	PM546	**1**	**6**	**12**	**14**	PM567	**2**	**7**	**11**	**13**	PM597	**3**	**8**	PM605	**4**	**9**	PM650	**5**	**10**
F_3-ethanol[a]		39	47	40		30	47	49	45	39	56	54	58	51	57	61	27	33	38
Methanol		45	58	49	5	34	54	58	53	48	54	52	60	55	58	60	12	27	31
Ethanol		44	56	50	7	36	52	59	57	51	51	52	59	56	60	64		21	25
Ethyl acetate	23	43	53	59	16	48	63	68	61	59	53	59	65	55	60	67	35	50	55
Acetone	14	37		52	14	36	55	57	60	55	50	53	60	57	59	65	31	44	49

[a] F_3-ethanol: 2,2,2,-trifluoroethanol

than compounds **1**–**4**. In the compounds **7**–**9**, the highest lasing efficiencies (an impressive 65-67%) are obtained in ethyl acetate, which is the solvent where those dyes have the highest quantum yield and radiative rate constant as well as the lowest nonradiative rate constant. In compound **6**, the highest quantum yield and radiative rate constant and the lowest nonradiative rate constant are achieved in methanol, and thus it is in this solvent where the highest lasing efficiency (58%) is observed.

The derivatives of PM567 with acryloyloxy (**11**) and methoxy (**13)** groups do not improve the lasing efficiencies demonstrated with the trifluoroacetoxy derivative **7**, in accordance with their lower fluorescence quantum yields and higher nonradiative rate constants, albeit compound **11** improves slightly de emission efficiency of derivative **2**, also in agreement with the slightly better photophysical parameters of**11** as compared with **2** (Table S2 in the Supporting Information). In the group of dyes pumped at 355 nm, compound **12**, derivative of PM546 incorporating propiloyloxy groups, exhibits much higher lasing efficiencies than the parent dye and the other derivatives, with the exception of compound **6**, which has better laser emission in polar protic solvents. This behavior reflects the photophysical properties: as can be seen in Table S1 in the Supporting Information, in polar protic solvents **6** has higher quantum yields and lower nonradiative constants than **12**, but the contrary happens in polar aprotic solvents. Compound **14**, on the other hand, is the one with the poorest lasing performance as a result of the fluorescence quenching processes discussed above, when considering the photophysical properties of the new derivatives.

Regarding dye PM650 and its derivatives **5** and **10**, as we have discussed in the previous section their emission properties are limited by the presence of an ICT state, which results in low fluorescence quantum yields in polar media. As a result their lasing efficiencies are lower than those of the other compounds pumped at 532 nm. As seen in Table S5 (Supporting Information), the fluorescence performance of these dyes is somewhat improved in polar aprotic solvents, which correlates with their higher lasing efficiencies in ethyl acetate and acetone, as compared with those observed in F_3-ethanol, methanol and ethanol.

An important parameter for any practical application of the dye lasers is their lasing photostability under repeated pumping. In Table 3 are collected data on the decrease of the laser-induced fluorescence intensity, under transversal excitation of capillary containing dye solutions in ethyl acetate (see Experimental Section), after a given number *n* of pump pulses, for both the commercial dyes and their derivatives synthesized in the present work. Dye PM546 and its derivatives **1** and **6** were pumped at 355 nm and 5 Hz repetition rate. All the other dyes were pumped at 532 nm and 10 Hz repetition rate. The pump energy was in all cases 5 mJ.

It has to be remarked that all the newly synthesized *O*-BODIPYs are more photostable than the corresponding *F*-BODIPYs, with the exception of **14** and derivatives of PM650, which lower stability reflects their lower chemical stability, due to the mechanism discussed above, when analyzing their photophysical properties.

2.3.2. Bulk Solid State

The excellent laser performance exhibited by the new dyes in liquid solution led us to explore their behavior as photonic materials, either in bulk as SSDLs or incorporated into waveguiding structures. To this end, as a proof of concept, we chose dye PM567 as reference with which to compare the laser behavior of derivatives **2** and **7** under identical experimental conditions. As matrix material we chose PMMA because it mimics ethyl acetate, the solvent in which those dyes exhibited the highest lasing efficiencies in liquid solution (Table 4). The dye concentration in the matrix was that which optimized the lasing efficiency in ethyl acetate (Table 3). We have seen in previous work[18] that the covalent bonding of the chromophore to the polymeric matrix improves significantly the dye photostability because new channels are open to dissipate the excess energy released to the medium as heat. To check out the effect of this mechanism in the present case, PMMA matrices were also prepared incorporating dye **11**, which is an *O*-derivative of PM567 with acrylic bonds that allow the covalent bonding of the dye to the polymeric chains.

Table 5. Lasing properties of dyes incorporated in solid PMMA matrices. Eff: lasing efficiency; λ_l: peak laser emission wavelength; I_n(%): intensity of the laser output after *n* pump pulses in the same position of the sample, $I_n(\%) = 100(I_n/I_0)$, where I_0 is the initial intensity.

Dye	Eff [%]	λ_l [nm]	I_{100000} [%][a)]	I_n [%][b)]	*n*
PM567	34	566	30	0	12000
2	49	568	80	0	40000
7	56	568	100	80	100000
11	47	567	100	0	100000

[a)]Pumping at 10 Hz; [b)]Pumping at 30 Hz.

Table 5 collects the lasing performance of the different dyes. The lasing efficiencies of the new materials based on PMMA doped with*O*-BODIPYs enhance significantly those recorded with the commercial PM567 and correlate with those obtained in liquid solution, with the efficiency of dye **7** being the highest and being maintained the relationship: Eff (PM567) < Eff (**11**) < Eff (**2**) < Eff (**7**). These efficiencies are lower than those obtained in liquid solution, probably due to the fact that the finishing of the surface of the solid samples relevant to the laser operation was not laser-grade, so that higher efficiencies are to be expected with laser-grade surfaces.

To assess the photostability of the new materials we followed the evolution of their laser emission under repeated pumping in the same position of the sample at 10 Hz repetition rate. All the three derivatives demonstrated a much higher photostability than the parent dye PM567 (Table 5). After 100 000 pump pulses, the emission of compound **2** dropped by 20%, but the lasing intensity of both derivatives **7** and **11** remained constant at the initial level. Trying to distinguish more clearly the photostability behavior of the different dyes, we decided to subject the dyes to more drastic pumping conditions. We had demonstrated in previous work that the accumulation of heat into polymeric SSDLs increases significantly with the pumping repetition rate, resulting in a decrease in the lasing photostability.[19] Consequently, we proceeded to pump the SSDLs at 30 Hz repetition rate. The results are collected in the last two columns of Table 5. To facilitate comparison of the results obtained in a more intuitive way, the actual evolution of the

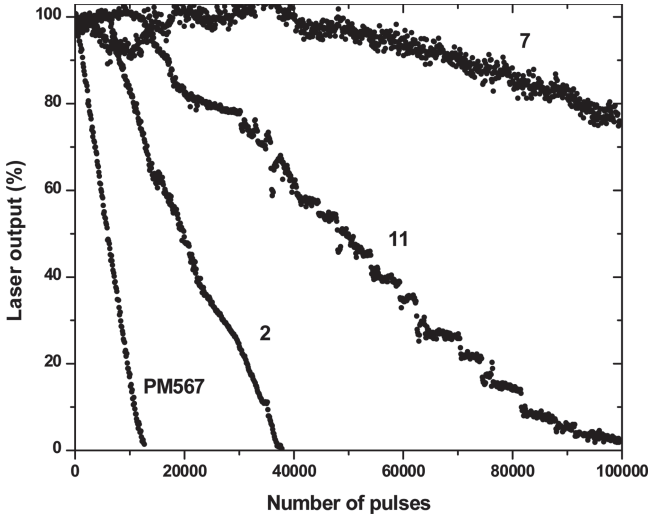

Figure 5. Normalized laser output as a function of the number of pump pulses in the same position of the sample of parent dye PM567 and its derivatives **2**, **7** and **11**. Pump energy and repetition rate: 3.5 mJ pulse^{-1} and 30 Hz, respectively.

laser emission of the different dyes at 30 Hz repetition rate is showed in **Figure 5**.

Compound **11** being covalently bonded to the polymeric chains improves the heat dissipation and, consequently, the lasing photostability with respect to dye **2**, which is merely solved into the matrix. However, the highest photostability is achieved with PMMA doped with dye **7**, with a drop in its emission intensity of just 20% after 100,000 pump pulses. These unexpected results can be understood in the light of the photophysics of compounds **7** and **11** (Table S2 in the Supporting Information). While the fluorescence quantum yield and radiative rate constant of compound **7** in ethyl acetate are just somewhat higher than those of compound **11**, the nonradiative rate constant of **7** is much lower than that of **11**. That means that the energy not converted into laser emission, which appears in the medium as heat, is much lower in **7** than in **11**, which more than compensates the higher dissipation rates in the matrix doped with the covalently bonded dye **11**.

2.3.3. Thin Films

In the previous section, we have studied the laser properties of the newly synthesized dyes operated as conventional two-mirror lasers. Nevertheless, there has been significant work over the last few years exploring the development of organic thin film lasers based on dye doped polymers because of their potential applications as coherent light sources suitable for integration in optoelectronic and disposable spectroscopic and sensing devices.[1d] In order to explore the suitability of the newly synthesized dyes for integrated devices, we implemented distributed feedback (DFB) lasers, the most common resonator type for organic thin film lasers.[1a]

In DFB lasers, light propagating in a waveguide mode of the organic film is Bragg-scattered by a wavelength-scale periodic modulation of the refractive index in the film, substrate, or both, to create a diffracted wave propagating in the counter propagating waveguide mode. The propagating and counter propagating modes will destructively interfere with each other at a given wavelength to create a photonic stopband at which light propagation is forbidden. This optical gap, whose width depends on the refractive index contrast of the periodic modulation, is centered at a wavelength λ_B, satisfying the Bragg condition, $m\lambda_B = 2\, n_{eff}\Lambda$, where m is an integer that represents the order of the diffraction, n_{eff} is the effective refractive index of the waveguide, which represents a geometrical average of the refractive indices of the three layers of the waveguide, and Λ is the period of the modulation.[1a] Working with the second order $m = 2$, the resonant wavelength is equal to $n_{eff}\Lambda$, and light is diffracted out of the surface of the film perpendicular to the plane of the waveguide. That is, the second-order structure provides a surface-emitted output coupling of the laser light via first-order diffraction while providing in-plane feedback via second-order diffraction (Figure S7a in Supporting Information).

The fundamental transverse electric (TE_0) propagating mode in a waveguide 1 μm thick with refractive index 1.4900 (PMMA), deposited onto a quartz substrate ($n = 1.456$), experiences an effective refractive index $n_{eff} \approx 1.477$, as calculated with a waveguide mode solver,[20] in the range 550-600 nm. Hence, if dye doped PMMA thin films are deposited on substrates with modulation periods $\Lambda_1 = 386$ nm and $\Lambda_2 = 400$ nm, second-order photonic stopbands centered at $\lambda_{B1} \approx 570$ nm and $\lambda_{B2} \approx 590$ nm, respectively, will be obtained. As λ_{B1} and λ_{B2} match the emission windows of the PM567 and PM597 families, respectively, we choose these dyes to implement the DFB lasers.

Two compounds of each family were chosen, the commercial compounds as the references and the derivatives with trifluoroacetoxy groups (compounds **7** and **8**), which showed the best laser performances both in liquid and bulk media. In order to better compare the laser performances, the dye concentrations were selected to render similar absorbance (Abs ≈ 0.055) at the pumping wavelength (532 nm), enough to provide the needed gain while avoiding the undesirable effects of dye aggregation.

In agreement with the estimated Bragg resonant wavelengths, when the devices were pumped well above threshold DFB laser emission was obtained around 570 nm, for samples with PM567 and **7**, and around 590 nm, for samples with PM597 and **8** (**Figure 6**a).

Explicitly, the laser peaks were centered at 569.3 nm for PM567, 571.6 nm for **7**, 589.3 nm for PM597 and 590.4 nm for **8**. The differences in the emission wavelengths between each group of samples have its origin in the slight differences in the sample thicknesses, which modifies the effective refractive indexn_{eff} and, in turn, the resonant wavelength.

Figure 6b,c show the dependence of the DFB emission intensity on the pump intensity for the samples doped with PM567 derivatives and PM597 derivatives, respectively. At low pump intensities there is just fluorescence and the emission grows linearly. Once the threshold is reached, the intensity of the emission grows superlinearly with the pump intensity, and the emission linewidth collapses to a mere 0.2 nm (Figure 6a). From the data in Figure 6b it is seen that the sample with **7** not only has a lower laser threshold than that with PM567 (1.7 against 2.5 kW cm^{-2}) but presents an output intensity up to an order of magnitude higher, in agreement with the results

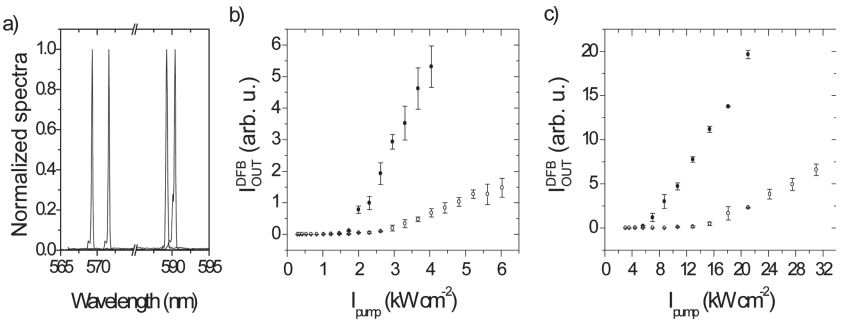

Figure 6. a) From left to right, DFB laser spectra of commercial PM567, derivative **7**, commercial PM597 and derivative **8** doped in PMMA. b) Output intensity as a function of pump intensity for commercial PM567 35 mM (hollow circles) and derivative **7** 25 mM (filled circles) doped in PMMA. c) Output intensity as a function of pump intensity for commercial PM597 25 mM (hollow circles) and derivative **8** 30 mM (filled circles) doped in PMMA.

observed in bulk media. Analogous results are obtained when comparing the samples with **8** and PM597 (Figure 6c). In this case the sample with **8** presents a laser threshold of 6 kW cm^{-2}, to be compared to the 14.5 kW cm^{-2} needed to excite laser emission in the sample with PM597.

3. Experimental Section

BODIPY dyes PM546, PM567, PM597, PM605 and PM650 were purchased from Lasing, S. A. and used as received.[12] New BODIPYs **1–12** and **14** were synthesized by modification of methods previously described.[8a,11] Compound **13**[6f] was synthetized according to procedure described in the literature.

Characterization of the new dyes as well as quantum mechanical simulations, preparation of laser samples, methods followed to analyze the photophysical and laser properties in liquid and solid phase and procedures to pH and solubility studies are described in detail in the Supporting Information.

4. Conclusions

The development of *O*-BODIPYs from commercial dyes is a successful strategy to obtain optimized laser dyes. The replacement of the fluorines by electron acceptor carboxylate groups ameliorate the fluorescence efficiency, reaching in some cases values around 100%; hence, these novel BODIPYs would be promising candidates to achieve tunable lasers at different regions of the visible with improved performance. To confirm this possibility, the lasing performance of the new derivatives in liquid solution and solid state was assessed and compared with that of the parent dyes.

The lasing efficiencies of the new compounds correlate well with their photophysical properties: all the derivatives exhibit a lasing efficiency higher than that of the commercial parent dye (except **14**, derivative of PM546 with aryloxy groups, in agreement with its lower fluorescence capability), with the highest lasing efficiencies being obtained in the derivatives incorporating trifluoroacetoxy groups.

To assess the laser behavior of the new dyes in solid state, dye PM567 and its derivatives **2**, **7**, and **11** were incorporated into solid matrices of PMMA. The lasing efficiencies of the *O*-BODIPYs were in all cases higher than that of the parent dye, and correlate with those obtained in liquid solution. Thus, the highest efficiency, 56%, was obtained with compound **7**. Compound **7** also exhibited a very high lasing stability, with the laser emission remaining at 80% of its initial value after 100 000 pump pulses in the same position of the sample at 30 Hz repetition rate.

DFB laser emission was demonstrated with organic films incorporating trifluoroacetoxy derivatives **7** and **8**, deposited onto quartz substrates engraved with appropriated periodical structures. Both derivatives exhibited laser thresholds lower than those of the parent dyes as well lasing intensities up to one order of magnitude higher. In view of the easy synthetic assembly, and the large number of described BODIPY laser dyes, we are confident that this powerful approach can be extended to other dyes of this family, furthering their practical application in optical and sensing fields.[21]

Supporting Information

Supporting Information is available from the Wiley Online Library or from the author.

Acknowledgements

This work was supported by Projects MAT2010-20646-C04-01, MAT2010-20646-C04-02, MAT2010-20646-C04-04 and TRACE 2009-0144 of the Spanish Ministerio de Ciencia e Innovación (MICINN), actually Spanish Ministerio de Economia y Competitividad (MINECO). I.E. thanks the Gobierno Vasco for a predoctoral contract IT339-10. L.C., M.E.P.-O. and G.D.-S. thank MICINN for a predoctoral scholarship (FPI, cofinanced by Fondo Social Europeo).

Received: January 17, 2013
Revised: February 6, 2013
Published online: March 26, 2013

[1] a) I. D. W. Samuel, G. A. Turnbull, *Chem. Rev.* **2007**, *107*, 1272; b) H. Zou, S. Wu, J. Shen, *Chem. Rev.* **2008**, *108*, 3893; c) D. Bera, L. Qian, T.-K. Tseng, P. H. Holloway, *Materials* **2010**, *3*, 2260; d) C. Grivas, M. Pollnau, *Laser Photonics Rev.* **2012**, *6*, 419.

[2] a) A. Costela, I. García-Moreno, R. Sastre, in *Tunable Laser Applications*, (Ed: F. J. Duarte), CRC Press, Boca Raton, FL**2009**, Ch. *3*, pp 97–120; b) O. García, L. Garrido, R. Sastre, A. Costela, I. García-Moreno, *Adv. Funct. Mater.* **2008**, *18*, 2017; c) O. García, R. Sastre, I. García-Moreno, V. Martín, A. Costela, *J. Phys. Chem. C* **2008**, *112*, 14710; d) I. García-Moreno, A. Costela, V. Martín, M. Pintado-Sierra, R. Sastre, *Adv. Funct. Mater.* **2009**, *19*, 2547; e) A. Costela, I. García-Moreno, L. Cerdán, V. Martín, O. García, R. Sastre, *Adv. Mater.* **2009**, *21*, 4163; f) L. Cerdán, A. Costela, I. García-Moreno, O. García, R. Sastre, D. Muñoz, J. de Abajo, *Macromol. Chem. Phys* **2009**, *210*, 1624; g) R. Sastre, V. Martín, L. Garrido, J. L. Chiara, B. Trastoy, O. García, A. Costela, I. García-Moreno, *Adv. Funct. Mater.* **2009**, *19*, 3307; h) E. Enciso, A. Costela,

I. García-Moreno, V. Martín, R. Sastre, *Langmuir* **2010**, *26*, 6154; i) L. Cerdán, A. Costela, I. García-Moreno, O. García, R. Sastre, *Opt. Express* **2010**, *18*, 10247; j) V. Martín, J. Bañuelos, E. Enciso, I. López Arbeloa, A. Costela, I. García-Moreno, *J. Phys. Chem. C* **2011**, *115*, 3926; k) M. E. Pérez-Ojeda, C. Thivierge, V. Martín, A. Costela, K. Burgess, I. García-Moreno, *Opt. Mater. Express* **2011**, *1*, 243; l) M. E. Pérez-Ojeda, B. Trastoy, I. López Arbeloa, J. Bañuelos, A. Costela, I. García-Moreno, J. L. Chiara, *Chem. Eur. J* **2011**, *17*, 13258; m) L. Cerdán, A. Costela, G. Durán-Sampedro, I. García-Moreno, M. Calle, J. de Abajo, G. A. Turnbull, *J. Mater. Chem.* **2012**, *22*, 8938; n) L. Cerdán, A. Costela, I. García-Moreno, *Org. Electron.* **2012**, *13*, 1463; o) L. Cerdán, A. Costela, I. García-Moreno, J. Bañuelos, I. López Arbeloa, *Laser Phys. Lett.* **2012**, *9*, 426; p) L. Cerdán, E. Enciso, V. Martín, J. Bañuelos, I. López Arbeloa, A. Costela, I. García-Moreno, *Nat. Photonics* **2012**, *6*, 621; q) L. Cerdán, A. Costela, G. Durán-Sampedro, I. García-Moreno, *Appl. Phys. B* **2012**, *108*, 839.

[3] a) T. G. Pavlopoulos, M. Shah, J. H. Boyer, *Appl. Opt.* **1988**, *27*, 4998; b) M. Shah, K. Thangaraj, M. L. Soong, L. T. Wolford, J. H. Boyer, I. R. Politzer, T. G. Pavlopoulos, *Heteroatom. Chem.* **1990**, *1*, 389; c) T. G. Pavlopoulos, J. H. Boyer, M. Shah, K. Thangaraj, M. L. Soong, *Appl. Opt.* **1990**, *29*, 3885; d) T. G. Pavlopoulos, J. H. Boyer, K. Thangaraj, G. Sathyamoorthi, M. P. Shah, M. L. Soong, *Appl. Opt* **1992**, *31*, 7089; e) J. H. Boyer, A. M. Haag, G. Sathyamoorthi, M. L. Soong, K. Thangaraj, T. G. Pavlopoulos, *Heteroatom. Chem* **1993**, *4*, 39.

[4] a) F. Lopez Arbeloa, J. Bañuelos, V. Martinez, T. Arbeloa, I. Lopez Arbeloa, *Int. Rev. Phys. Chem.* **2005**, *24*, 339; b) O. Garcia, R. Sastre, D. del Agua, A. Costela, I. Garcia-Moreno, *Chem. Mater.* **2006**, *18*, 601; c) I. Garcia-Moreno, F. Amat-Guerri, M. Liras, A. Costela, L. Infantes, R. Sastre, F. Lopez Arbeloa, J. Bañuelos Prieto, I. Lopez Arbeloa, *Adv. Funct. Mater.* **2007**, *17*, 3088; d) A. Costela, I. Garcia-Moreno, M. Pintado-Sierra, F. Amat-Guerri, R. Sastre, M. Liras, F. Lopez Arbeloa, J. Bañuelos Prieto, I. Lopez Arbeloa, *J. Phys. Chem. A* **2009**, *113*, 8118; e) M. J. Ortiz, I. Garcia-Moreno, A. R. Agarrabeitia, G. Duran-Sampedro, A. Costela, R. Sastre, F. Lopez Arbeloa, J. Bañuelos Prieto, I. Lopez Arbeloa, *Phys. Chem. Chem. Phys.* **2010**, *12*, 7804; f) J. Bañuelos Prieto, A. R. Agarrabeitia, I. Garcia-Moreno, I. Lopez-Arbeloa, A. Costela, L. Infantes, M. E. Perez-Ojeda, M. Palacios-Cuesta, M. J. Ortiz, *Chem. Eur. J.* **2010**, *16*, 14094; g) Y. Xiao, D. Zhang, X. Qian, A. Costela, I. Garcia-Moreno, V. Martin, M. E. Perez-Ojeda, J. Bañuelos, L. Gartzia, I. Lopez Arbeloa, *Chem. Commun.* **2011**, *47*, 11513; h) J. Bañuelos, V. Martin, C. F. A. Gomez-Duran, I. J. Arroyo Cordoba, E. Peña-Cabrera, I. Garcia-Moreno, A. Costela, M. E. Perez-Ojeda, T. Arbeloa, I. Lopez Arbeloa, *Chem. Eur. J.* **2011**, *17*, 7261; i) G. Duran-Sampedro, A. R. Agarrabeitia, I. Garcia-Moreno, A. Costela, J. Bañuelos, T. Arbeloa, I. López Arbeloa, J. L. Chiara, M. J. Ortiz, *Eur. J. Org. Chem.* **2012**, *32*, 6335.

[5] a) A. Loudet, K. Burgess, *Chem. Rev.* **2007**, *107*, 4891; b) R. Ziessel, G. Ulrich, A. Harriman, *New J. Chem.* **2007**, *31*, 496; c) G. Ulrich, R. Ziessel, A. Harriman, *Angew. Chem. Int. Ed.* **2008**, *47*, 1184; d) F. L. Arbeloa, J. Bañuelos, V. Martinez, T. Arbeloa, I. L. Arbeloa, *Trends Phys. Chem.* **2008**, *13*, 101; e) A. C. Benniston, G. Copley, *Phys. Chem. Chem. Phys.* **2009**, *11*, 4124; f) M. Benstead, G. H. Mehl, R. W. Boyle, *Tetrahedron* **2011**, *67*, 3573; g) N. Boens, V. Leen, W. Dehaen, *Chem. Soc. Rev.* **2012**, *41*, 1130; h) S. G. Awuah, Y. You, *RSC Adv.* **2012**, *2*, 11169; i) A. Kamkaew, S. H. Lim, H. B. Lee, L. V. Kiew, L. Y. Chung, K. Burgess, *Chem. Soc. Rev.* **2013**, *42*, 77.

[6] a) L. Li, B. Nguyen, K. Burgess, *Bioorg. Med. Chem. Lett.* **2008**, *18*, 3112; b) C. Bonnier, W. E. Piers, A. Al-Sheikh Ali, A. Thompson, M. Parvez, *Organometallics* **2009**, *28*, 4845; c) S. M. Crawford, A. Thompson, *Org. Lett.* **2010**, *12*, 1424; d) T. W. Hudnall, T.-P. Lin, F. P. Gabbaï, *J. Fluorine Chem.* **2010**, *131*, 1182; e) G. Ulrich, S. Goeb, A. De Nicola, P. Retailleau, R. Ziessel, *J. Org. Chem.* **2011**, *76*, 4489; f) L. Yang, R. Simionescu, A. Lough, H. Yan, *Dyes Pigments* **2011**, *91*, 264; g) T. Lundrigan, S. M. Crawford, T. S. Cameron, A. Thompson, *Chem. Commun.* **2012**, *48*, 1003; h) T. Lundrigan, A. Thompson, *J. Org. Chem.* **2012**, *78*, 757.

[7] a) L. Bonardi, G. Ulrich, R. Ziessel, *Org. Lett.* **2008**, *10*, 2183; b) A. Nagai, J. Miyake, K. Kokado, Y. Nagata, Y. Chujo, *J. Am. Chem. Soc.* **2008**, *130*, 15276; c) A. Harriman, L. Mallon, R. Ziessel, *Chem. Eur. J.* **2008**, *14*, 11461; d) T. Rousseau, A. Cravino, T. Bura, G. Ulrich, R. Ziessel, J. Roncali, *Chem. Commun.* **2009**, 1673; e) A. Harriman, L. J. Mallon, K. J. Elliot, A. Haefele, G. Ulrich, R. Ziessel, *J. Am. Chem. Soc.* **2009**, *131*, 13375; f) J.-H. Olivier, A. Haefele, P. Retailleau, R. Ziessel, *Org. Lett.* **2010**, *12*, 408; g) T. Bura, P. Retailleau, R. Ziessel, *Angew. Chem. Int. Ed.* **2010**, *49*, 6659; h) T. Bura, R. Ziessel, *Org. Lett.* **2011**, *13*, 3072; i) S. Rihn, M. Erdem, A. De Nicola, P. Retailleau, R. Ziessel, *Org. Lett.* **2011**, *13*, 1916; j) S. Zhu, N. Dorh, J. Zhang, G. Vegesna, H. Li, F.-T. Luo, A. Tiwari, H. Liu, *J. Mater. Chem.* **2012**, *22*, 2781; k) J.-S. Lu, S.-B. Ko, N. R. Walters, S. Wang, *Org. Lett.* **2012**, *14*, 5660.

[8] a) C. Tahtaoui, C. Thomas, F. Rohmer, P. Klotz, G. Duportail, Y. Mély, D. Bonnet, M. Hibert, *J. Org. Chem.* **2007**, *72*, 269; b) Y. Tokoro, A. Nagai, Y. Chujo, *Tetrahedron Lett.* **2010**, *51*, 3451; c) C. A. Wijesinghe, M. E. El-Khouly, N. K. Subbaiyan, M. Supur, M. E. Zandler, K. Ohkubo, S. Fukuzumi, F. D'Souza, *Chem. Eur. J.* **2011**, *17*, 3147; d) B. Brizet, A. Eggenspiller, C. P. Gros, J. M. Barbe, C. Goze, F. Denat, P. D. Harvey, *J. Org. Chem.* **2012**, *77*, 3646.

[9] a) A. K. Parhi, M.-P. Kung, K. Ploessl, H. F. Kung, *Tetrahedron Lett.* **2008**, *49*, 3395; b) C. Ikeda, S. Ueda, T. Nabeshima, *Chem. Commun.* **2009**, 2544; c) A. Kubo, Y. Minowa, T. Shoda, K. Takeshita, *Tetrahedron Lett.* **2010**, *51*, 1600; d) S. Rausaria, A. Kamadulski, N. P. Rath, L. Bryant, Z. Chen, D. Salvemini, W. L. Neumann, *J. Am. Chem. Soc.* **2011**, *133*, 4200; e) Y. Tomimori, T. Okujima, T. Yano, S. Mori, N. Ono, H. Yamada, H. Uno, *Tetrahedron* **2011**, *67*, 3187.

[10] a) C. Bonnier, W. E. Piers, M. Parvez, T. S. Sorensen, *Chem. Commun.* **2008**, 4593; b) C. Bonnier, W. E. Piers, M. Parvez, *Organometallics* **2011**, *30*, 1067.

[11] X.-D. Jiang, J. Zhang, T. Furuyama, W. Zhao, *Org. Lett.* **2012**, *14*, 248.

[12] Laser grade, Exciton. They were used as received with a purity >99%.

[13] C. Hansch, A. Leo, R. W. Taft, *Chem. Rev.* **1991**, *91*, 165.

[14] G. Bourhill, J.-L. Brédas, L-T. Cheng, S. R. Marder, F. Meyers, J. W. Perry, B. G. Tiemann, *J. Am. Chem. Soc.* **1994**, *116*, 2619.

[15] I. Esnal, J. Bañuelos, I. López Arbeloa, A. Costela, I. García-Moreno, M. Garzón, A. R. Agarrabeitia, M. J. Ortiz, *RSC Adv.* **2013**, *3*, 1547.

[16] J. Bañuelos, T. Arbeloa, M. Liras, V. Martinez, F. López Arbeloa, *J. Photochem. Photobiol. A* **2006**, *184*, 298.

[17] a) A. P. de Silva, H. Q. N. Gunaratne, T. Gunnlaugsson, A. J. M. Huxley, C. P. McCoy, J. T. Rademacher, T. E. Rice, *Chem. Rev.* **1997**, *97*, 1515; b) K. Rurack, U. Resch-Genger, *Chem. Soc. Rev.* **2002**, *31*, 116; c) H. Sunahara, Y. Urano, H. Kojima, T. Nagano, *J. Am. Chem. Soc.* **2007**, *129*, 5597; d) J. Bañuelos, I. J. Arroyo-Cordoba, I. Valois-Escamilla, A. Alvarez-Hernández, E. Peña-Cabrera, R. Hu, B. Z. Tang, I. Esnal, V. Martínez, I. López Arbeloa, *RSC Adv.* **2011**, *1*, 677.

[18] A. Costela, I. García-Moreno, R. Sastre, *Phys. Chem. Chem. Phys.* **2003**, *5*, 4745.

[19] a) A. Costela, I. García-Moreno, D. del Agua, O. García, R. Sastre, *Appl. Phys. Lett.* **2004**, *85*, 2160; b) A. Costela, I. García-Moreno, D. del Agua, O. García, R. Sastre, *J. Appl. Phys.* **2007**, *101*, 073110.

[20] Online 1D multilayer slab waveguide mode solver by Dr. Manfred Hammer. http://wwwhome.math.utwente.nl/_hammer/oms.html (accessed March 2013).

[21] M. J. Ortiz, A. R. Agarrabeitia, M. Garzón Sanz, I. García-Moreno, A. Costela, G. Durán-Sampedro, Spanish Patent Application no. 201200871, **2012**.